

Published in final edited form as:

FASEB J. 2008 June ; 22(6): 1660. doi:10.1096/fj.07-092841.

Selective targeting of the $\gamma 1$ isoform of protein phosphatase 1 to F-actin in intact cells requires multiple domains in spinophilin and neurabin

Leigh C. Carmody^{*}, Anthony J. Baucum II^{*,†}, Martha A. Bass^{*}, and Roger J. Colbran^{*,†}

^{*} Department of Molecular Physiology and Biophysics, Vanderbilt University School of Medicine, Nashville, Tennessee 37232-0615, USA

[†] The Center for Molecular Neuroscience, and [†] The Vanderbilt Kennedy Center for Research on Human Development, Vanderbilt University School of Medicine, Nashville, Tennessee 37232-0615, USA

Abstract

Protein phosphatase 1 (PP1) catalytic subunits dephosphorylate specific substrates in discrete subcellular compartments to modulate many cellular processes. Canonical PP1-binding motifs (R/K-V/I-X-F) in a family of proteins mediate subcellular targeting, and the amino acids that form the binding pocket for the canonical motif are identical in all PP1 isoforms. However, PP1 $\gamma 1$, but not PP1 β , is selectively localized to F-actin rich dendritic spines in neurons. Although the F-actin-binding proteins neurabin I and spinophilin (neurabin II) also bind PP1, their role in PP1 isoform selective targeting in intact cells is poorly understood. We show here that spinophilin selectively targets PP1 $\gamma 1$, but not PP1 β , to F-actin-rich cortical regions of intact cells. Mutation of a PP1 $\gamma 1$ selectivity determinant (N⁴⁶⁴EDYDRR⁴⁷⁰ in spinophilin: conserved as residues 473–479 in neurabin) to **VKDYDTW** severely attenuated PP1 $\gamma 1$ interactions with neurabins *in vitro* and in cells, and disrupted PP1 $\gamma 1$ targeting to F-actin. This domain is not involved in the weaker interactions of neurabins with PP1 β . In contrast, mutation of the canonical PP1 binding motif attenuated interactions of neurabins with both isoforms. Thus, selective targeting of PP1 $\gamma 1$ to F-actin by neurabins in intact cells requires both the canonical PP1-binding motif and an auxiliary PP1 $\gamma 1$ -selectivity determinant.

Keywords

Subcellular targeting; cytoskeleton; dendritic spine; synaptic plasticity

Introduction

Four protein phosphatase 1 (PP1) catalytic subunit isoforms (α , β , $\gamma 1$ and $\gamma 2$)¹ are $\approx 80\%$ identical in amino acid sequence and are major serine/threonine phosphatases in mammalian cells (reviewed in (1)). The PP1 catalytic subunits are targeted to discrete subcellular compartments and regulated by interactions with >50 proteins that typically contain a canonical PP1 binding motif with a consensus R/K-V/I-X-F sequence (2,3). Residues that form the binding pocket for the canonical motif are identical in the four isoforms, yet the PP1 isoforms

Address for correspondence: Roger J. Colbran, Ph.D., Room 724 Robinson Research Building, Vanderbilt University Medical Center, Nashville, TN 37232-0615. Phone: (1) 615-936-1630. FAX: (1) 615-322-7236. roger.colbran@vanderbilt.edu.

¹A single PP1 isoform has been referred to as both PP1 β and PP1 δ in the literature, depending on the species and lab of origin. Herein, we identify this isoform as PP1 β to be consistent with our previous work.

exhibit distinct subcellular localizations. For example, in neurons, PP1 β is enriched in the soma and in the dendritic shaft, whereas PP1 α and PP1 γ 1 are enriched in dendritic spines (4–6). Peptides that non-specifically disrupt PP1 catalytic subunit interactions with canonical binding motifs profoundly regulate excitatory synaptic transmission, suggesting that targeting of PP1, presumably to dendritic spines, is critical for normal modulation of synaptic plasticity (7–9). However, mechanisms underlying the isoform selectivity of PP1 targeting are unclear.

Dendritic spines are highly specialized F-actin rich protrusions on dendrites that contain neurabin I and spinophilin (neurabin II), related F-actin and PP1-binding proteins (10–16). The neurabins homo- and hetero-multimerize, and also bind many other proteins involved in regulating spine morphology and other cellular functions (17–22). Interestingly, neurabin, spinophilin, and many of their interacting partners are regulated by reversible protein phosphorylation, which can modulate assembly of the complex and/or activity of the associated proteins (reviewed in (23)). Therefore, neurabins modulate several signaling cascades by coordinating the assembly of multi-protein complexes that are regulated by phosphorylation.

The association of PP1 presumably plays a key role in modulating the function of neurabin complexes. Indeed, PP1 is perhaps the best-studied interaction partner of the neurabins. Stable binding of PP1 requires canonical PP1-binding motifs in spinophilin (K⁴⁴⁸IHF⁴⁵¹) and neurabin (K⁴⁵⁷IKF⁴⁶⁰) (10,24,25). Interestingly, biochemical studies have shown that both of the neurabins preferentially bind PP1 γ 1 over PP1 β (13,25,26). Moreover, spinophilin and neurabin are targeted to dendritic spines apparently by the N-terminal F-actin-binding domain (4–6,10–12,14,15). These data are consistent with the idea that neurabins selectively target PP1 γ 1 to the F-actin cytoskeleton in dendritic spines. However, the isoform selectivity of PP1 targeting by the neurabins in intact cells has not been established. Here we show that spinophilin selectively targets PP1 γ 1 to the F-actin cytoskeleton in intact cells and that targeting requires both the non-isoform selective canonical PP1-binding motif and an additional domain C-terminal to the canonical PP1-binding motif.

Materials and Methods

DNA Constructs

Spinophilin and neurabin mutations were generated from pCMV4-myc vectors containing cDNAs encoding the full-length rat proteins (13). Spinophilin F451A (Sp(F->A)) and neurabin F460A (Nb(F->A)) were generated using complementary forward (F) and reverse (R) primers containing the mutation: Sp(F->A) F: 5'-GCCCGAGCCGGAAGATCCATGCTAGCACCGCACCG-3'; and Nb(F->A) F: 5'-GCAAATAGGAAAATTAAGGCTAGCTGTGCTCCGATTAAG-3'. All other mutations were made using partially overlapping primer pairs in a two-step process, using methodology described by Zheng et al. (27). The first set of primers were as follows: Nb(VK) (N473V, E475K), F: 5'-GTACTCCGTAAAAGACTATGACAGG-3' and R: 5'-GTCTTTTACGGAGTACGTGTTGAAAAC-3'; Sp(VK) (Sp N464V, E465K), F: 5'-CCTACTCCGTTAAGGACTATG-3' and R: 5'-CATAGTCCTTAACGGAGTAGGTGCTGAATAC-3'. The initial mutant constructs were sequenced and then used as templates with a second set of primers: Nb(VK/TW) (N473V, E475K, R478T, R479W), F: 5'-CTCCGTTAAAGACTATGACACGTGGAATGATGACGTTG-3' and R: 5'-CATTCCACGTGTCATAGTCTTTAACGGAGTACGTGTTG-3'; Sp(VK/TW) (N464V, E465K, R469T, R470W), F: 5'-CTCCGTTAAGGACTATGACACATGGAATGAGGATGTGG-3' and R: 5'-CATTCCATGTGTCATAGTCCTTAACGGAGTAGGTGCTG-3'. Similarly, G_M(NE/RR) was generated in pGEX-4T-G_M (1–240) using two steps: GM(ND), (V79N, K80D), F: 5'-CTTTCTCATCGTTGGACACAAGATTGAATC-3' and R: 5'-

CTTTCTCATCGTTGGACACAAGATTGAATC-3'; GM(NE/RR), (V79N, K80E, T84R, W85R), F: 5'-GTGTGCGAACGAAGAGTTTGATAGGAGGG-3' and R: 5'-CAAACCTCTTCGTTTCGACACAAGATTGAATCC-3'. To create neurabin GST-fusion proteins, the full-length wild type neurabin or PP1 binding domain mutations (Nb F->A, Nb VK/TW) were used as templates to subclone residues 146–493 into pGEX-4T vector. The sequences of all constructs and mutations were confirmed by automated DNA-sequence analysis (GenHunter Corporation Sequencing (<http://www.genhunter.com/VUsequencing>), Nashville, TN). Eukaryotic expression vectors for N-terminal GFP-tagged PP1 γ 1 and PP1 β were generous gifts from Dr. Mattieu Bollen (Katholieke Universiteit, Leuven, Belgium) (28). The expression construct for the mCherry protein was a generous gift from the laboratory of Dr. D. Piston (Vanderbilt).

Antibodies

Rabbit and sheep antibodies recognizing the C termini of PP1 β or PP1 γ 1, and rabbit antibodies recognizing spinophilin and neurabin were described previously (5,13). Other antibodies were: mouse monoclonal PP2A (Transduction Laboratories), mouse monoclonal spinophilin (BD Pharmingen), mouse monoclonal neurabin (BD Pharmingen), mouse monoclonal GFP (Santa Cruz), mouse monoclonal myc (Zymed), donkey anti-mouse Cy5 (Jackson ImmunoResearch), donkey anti-rabbit Alexa594 (Invitrogen), donkey anti-mouse Alexa647 (Invitrogen).

Phosphatase Catalytic Subunit Preparation

A crude mixture of native protein phosphatase catalytic subunits was generated by ethanol precipitation of brain extracts, as previously described (13,29). The final preparations contained a mixture of monomeric phosphatase catalytic subunits, including an approximately equimolar ratio of PP1 β and PP1 γ 1, as determined by immunoblotting with isoform-selective antibodies in comparison with bacterial PP1 isoform standards (a generous gift of Dr. E.Y. Lee, New York Medical College). Native PP1 β and PP1 γ 1 were purified from the catalytic subunit preparation by adsorption to isoform-specific antibodies conjugated to Affi-Gel-10 (BioRad), eluted with sodium isothiocyanate, dialyzed, and then stored at -80°C in 50% glycerol (29).

Glutathione-agarose Co-sedimentation Assays

In the “standard” condition, the indicated GST fusion proteins (8 μg) were mixed for 1 hour at 4°C with the crude phosphatase catalytic subunit mixture (15 μg total protein) in a final volume of 1 ml binding buffer (50 mM Tris-HCl, pH 7.5, 0.2 M NaCl, 0.1% Triton X-100, 0.25 mg/ml bovine serum albumin). The final concentration of GST fusion protein (≈ 130 nM) was in excess of the approximate concentrations of PP1 β and PP1 γ 1 (≈ 25 nM each). Cosedimentation assays were also performed using a “stringent” protocol in which the entire incubation was diluted 14-fold in the same buffer. GST protein complexes were immunoblotted for the presence of phosphatase catalytic subunits as previously described (26,29).

PP1 Inhibition Assays

Activities of purified native PP1 isoforms were measured towards [^{32}P]phosphorylase *a* substrate, essentially as previously described (13,26,29).

Cell Culture and Transfections

293FT cells (Invitrogen) were transfected using FuGENE 6 (Roche Applied Science) with one or more constructs. Transfected cells were grown in 100-mm dishes for 40–48 h, lysed with 600 μl lysis buffer (50 mM Tris-HCl, pH 7.5, 120 mM NaCl, 1 mM EDTA, 0.1% (v/v) NP-40, 0.1% (w/v) deoxycholate, 0.1 mM PMSF, 1 mM benzamide, 20 mg/liter soybean trypsin

inhibitor, and 5 mg/liter leupeptin), sonicated, and then centrifuged ($5,000 \times g$, 10 minutes) to generate soluble cell extracts. Extracts were stored at -80°C until required.

Co-immunoprecipitations

293FT cell lysates were diluted to 1 mg/ml protein in IP buffer (50 mM Tris-HCl, pH 7.5, 0.15 M NaCl, 1 mM EDTA, 0.5% (v/v) Triton X-100, 1 mM PMSF, 5 mg/liter leupeptin, 20 mg/liter soybean trypsin inhibitor, and 0.5 mM benzamidine). Lysates were incubated with the indicated rabbit antibodies or equivalent amounts of non-immune rabbit IgG for 2 hours at 4°C . GammaBind Plus-Sepharose (Amersham Biosciences) beads were added and incubated for an additional 2 hours. Resin was collected, and immune complexes and supernatants were analyzed by immunoblotting.

Fluorescent microscopy

HEK293 or 293FT cells (Invitrogen) were plated onto poly-D-lysine coated coverslips, and transfected (as above). After 40–48 hours, cells were fixed with 4% (v/v) paraformaldehyde and 4% (w/v) sucrose in PBS (10 minutes, 37°C) and permeabilized with PBS containing 0.1% (v/v) Triton X-100 for five minutes at room temperature, as described previously (5). Coverslips were incubated with DRAQ5 (Biostatus Ltd.) in PBS, or mouse myc antibodies (1:100 dilution) in a PBS solution containing 2% (v/v) in normal donkey serum in PBS and 0.01% (v/v) Tween 20. Washed coverslips were incubated with anti-mouse Cy5 (1:800), and/or rhodamine-phalloidin (Molecular Probes, 1:40). Coverslips were mounted with Aqua Poly/Mount (Polysciences, Inc.) and imaged using a LSM 510 META inverted confocal microscope (Zeiss). GFP and RFP (not shown) autofluorescence was assessed. Controls were performed to verify that primary and secondary antibodies were specific and that fluorescent signals were restricted to the appropriate channel. Microscope settings were optimized to capture both bright and dim images and the same setting were used to collect all images within each experimental condition. Images shown represent single optical sections (nominal $0.5\ \mu\text{m}$ thickness) from the center of the cells. Each experiment contained two separate transfections for each condition and 5–12 fields of view were selected for analysis of each condition. For GFP-PP1 γ 1 samples, fields of view were randomly chosen. Due to lower transfection efficiency/expression, it was not possible to randomly choose fields of view for GFP-PP1 β . Therefore, fields of view containing three or more GFP expressing cells were chosen for quantification. Acquired images were uniformly adjusted by linearly reassigning the values of pixel intensities to use the full 8-bit range (0–255) and then thresholded based on control cells not expressing the transfected protein using Metamorph software (Molecular Devices). Colocalization was scored as the percentage of thresholded GFP fluorescent pixels that overlap with thresholded rhodamine fluorescent pixels (% pixel overlap). An intensity ratio was then calculated to provide a measure of colocalization that included information about the relative amount of protein in the two pools. First, the % pixel overlap (green over red) was multiplied by the average GFP fluorescence signal intensity in those pixels. This value was then divided by the average GFP fluorescence signal intensity in the non-colocalized fraction multiplied by the % of non-overlapping pixels. The quantified data shown were calculated from the entire field and no correction was made for the presence of singly transfected cells, although a majority of cells were co-transfected (>80%). In preliminary experiments, limiting quantitative analyses to individually selected co-transfected cells did not improve our ability to distinguish targeting of GFP-PP1 isoforms by wild type and mutated spinophilins, so we performed quantitative analyses on entire fields of view (see above) to avoid the potential for operator bias in selecting individual cells. For display purposes only, the contrast settings were increased to be able to see both dim and bright objects.

Results

Spinophilin is a PP1 γ 1-selective targeting subunit in intact cells

As an initial step toward investigating mechanisms controlling the subcellular localization of PP1 isoforms, we transiently expressed PP1 γ 1 and PP1 β as GFP fusion proteins in HEK293 cells. In order to monitor overall cell morphology, cells were co-transfected with a soluble monomeric red fluorescent protein (mCherry), fixed, and then nuclei were stained with DRAQ5. As reported previously (28), confocal fluorescence microscopy revealed GFP-PP1 γ 1 is strongly clustered within the cell: GFP-PP1 γ 1 clusters partially overlap DRAQ5 in some cells, but appear to be predominantly peri-nuclear in HEK293 cells. Parallel studies showed that GFP-PP1 γ 1 is predominantly nuclear in HeLa cells (not shown). In contrast, GFP-PP1 β is more diffusely, if unevenly, distributed throughout the nucleus and cytosol in HEK293 cells (Fig. 1A) and HeLa cells (not shown). The overall morphology and size of HEK293 cells or HeLa cells was unaffected by expression of either GFP-PP1 isoform, as indicated by mCherry fluorescence (Fig. 1A and data not shown).

Neurabins have been proposed to function as PP1-isoform selective F-actin targeting proteins. Expression of GFP-spinophilin in HEK293 cells resulted in predominant localization of GFP to sub-membrane cortical regions, quite distinct from the localization of either GFP-PP1 β or GFP-PP1 γ 1 (Fig. 1A). The overall morphology of HEK293 and HeLa cells was unaffected by expression of GFP-spinophilin under these conditions.

For initial qualitative assessment of the effect of neurabins on PP1 localization, GFP-PP1 isoforms were co-expressed with myc-tagged spinophilin. Co-expression of myc-spinophilin had little effect on the generally diffuse distribution of GFP-PP1 β , and there was little overlap in their localization. In contrast, co-expression of myc-spinophilin resulted in the transition of GFP-PP1 γ 1 fluorescence from predominant intracellular clusters to mostly peripheral submembranous localization, strongly overlapping with myc-spinophilin (Fig. 1B). Quantitative data further supporting this interpretation and defining mechanisms for isoform-specific targeting are described below. Notably, the range of sizes and morphologies of HEK293 cells co-expressing myc-spinophilin and GFP-PP1 isoforms was not noticeably different from those expressing either protein alone. Co-expression of myc-neurabin resulted in noticeable, but only partial, redistribution of GFP-PP1 γ 1 from intracellular puncta, presumably because myc-neurabin was expressed at much lower levels than was myc-spinophilin (not shown). Taken together, these data directly demonstrate for the first time that neurabins preferentially target PP1 γ 1 over PP1 β in intact cells.

Neurabins contain multiple PP1-binding determinants

In order to investigate the mechanism for targeting PP1 γ 1 in cells, we first characterized the biochemical basis for selective interactions of PP1 isoforms with neurabins. Mutation of the phenylalanine residue within canonical PP1-binding motifs in spinophilin (K⁴⁴⁸IHF⁴⁵¹) and neurabin (K⁴⁵⁷IKF⁴⁶⁰) severely disrupts their interactions with PP1 (24,25). Our previous truncation studies showed that residues 473–479 of neurabin are necessary for selective binding of the PP1 γ 1 isoform *in vitro* (26). This PP1 γ 1 selectivity determinant is 100% conserved in spinophilin (residues 464–470) but critical residues within this domain were not identified. Therefore, we aligned amino acid sequences C-terminal to the canonical PP1 binding domain of spinophilin and neurabin with corresponding sequences from the muscle glycogen targeting subunit of PP1 (G_M)², which displays an inverse PP1 isoform selectivity (PP1 β > PP1 γ 1)

²The glycogen-binding PP1 subunit from striated muscle has been called either G_M or RGL 30.

Lanner, C., Suzuki, Y., Bi, C., Zhang, H., Cooper, L. D., Bowker-Kinley, M. M., and DePaoli-Roach, A. A. (2001) Gene structure and expression of the targeting subunit, RGL, of the muscle-specific glycogen-associated type 1 protein phosphatase, PP1G. *Archives of biochemistry and biophysics* **388**, 135–145.

(26). Four amino acids within the PP1 γ 1 selectivity determinant of the neurabins were not conserved in G_M (Figure 2A). Consequently, we mutated the NEDYDRR sequence in both neurabins to **VKDYDTW** (Nb(VK/TW) and Sp(VK/TW)).

GST fusion proteins containing the PP1 binding domain (residues 146–493) of neurabin (wild type: GST-Nb(WT). F460A mutant: GST-Nb(F->A). NEDYDRR to **VKDYDTW** mutant: GST-Nb(VK/TW)) were used in glutathione agarose cosedimentation assays to compare the effects of mutating the PP1 γ 1 selectivity determinant and the canonical PP1-binding motif. Parallel controls were performed with a GST fusion protein containing a fragment of G_M with inverse PP1 isoform binding selectivity (GST-G_M). Since recombinant PP1 isoforms do not typically display the full repertoire of biochemical properties of the native proteins (29,31), we tested the interactions of these protein fragments with native rat brain catalytic subunit isoforms. GST-Nb(WT) interacts with both PP1 β and PP1 γ 1 (Figure 2B), but preferentially interacts with PP1 γ 1 under our standard conditions (Figure 2B/C) (see Methods). Under more stringent conditions (i.e., with 14-fold dilution), the selectivity of GST-Nb(WT) for PP1 γ 1 becomes much more apparent (Figure 2D). This difference is not due to abnormal properties of the PP1 β preparation because GST-G_M selectively interacts with PP1 β rather than PP1 γ 1 (Fig. 2D). Mutation of either the canonical motif or the selectivity determinant completely prevented binding of PP1 γ 1 to GST-Nb under stringent incubation conditions (Figure 2D). Under “standard” conditions, mutation of the canonical binding motif greatly attenuated binding of both PP1 isoforms, but mutation of the selectivity determinant attenuated PP1 γ 1 binding without affecting the weaker binding of PP1 β (Figure 2B/C). These data identify residues Asn⁴⁷³, Glu⁴⁷⁴, Arg⁴⁷⁸, Arg⁴⁷⁹ as crucial determinants for stable binding of PP1 γ 1 to neurabin *in vitro*.

As an additional assessment of the effects of these mutations that does not require separation of complexes from excess unbound proteins, we assayed activities of purified native PP1 isoforms in the presence of various concentrations of the GST fusion proteins. GST-Nb(WT) is a much more potent inhibitor of PP1 γ 1 (EC_{50%} \approx 0.6 nM) than PP1 β (EC_{50%} \approx 40 nM) (Figure 3A), in agreement with previous studies (26). In contrast, GST-G_M preferentially inhibited PP1 β over PP1 γ 1, albeit only modestly (Figure 3D), consistent with previous studies. Mutation of the canonical binding motif in GST-Nb reduced the potency for inhibition of both isoforms by more than 100-fold, but it was readily apparent that the GST-Nb(F->A) retained similar selectivity for PP1 γ 1 as the parent GST-Nb(WT) protein (Figure 3B). In contrast, GST-Nb(VK/TW) exhibited no significant PP1 isoform selectivity (Figure 3C): the potency of PP1 γ 1 inhibition was decreased by \approx 100-fold, with only an \approx 2-fold affect on PP1 β inhibition (compare Figure 3A/C). These data show that the canonical binding motif is important for interaction of neurabin fragments with both PP1 isoforms, whereas specific residues (Asn⁴⁷³, Glu⁴⁷⁴, Arg⁴⁷⁸, Arg⁴⁷⁹) within a domain C-terminal to the canonical PP1-binding motif are critical only for high affinity interactions of neurabin fragments with PP1 γ 1.

Association of PP1 isoforms with the neurabins in cells

In order to investigate the relative importance of the canonical PP1-binding motif and the isoform selectivity determinant for binding of PP1 to full-length neurabins in intact cells, we compared the interaction of GFP-PP1 γ 1 with co-expressed myc-tagged wild type or mutated full-length versions of both proteins (WT, F->A, VK/TW). Initially, neurabin (myc-Nb) or spinophilin (myc-Sp) were immunoprecipitated from cell extracts and immune complexes were probed for PP1 γ 1. Both endogenous PP1 γ 1 and GFP-PP1 γ 1 co-precipitated with wild type neurabin (myc-Nb(WT)) (Figure 4A, lane 4) and wild type spinophilin (myc-Sp(WT)) (Figure 4B, lane 2). Neither form of PP1 γ 1 could be detected in immunoprecipitates of myc-Sp(F->A) mutant (canonical PP1-binding motif mutant) (Figure 4B, lane 4). However, small amounts of both endogenous PP1 γ 1 and GFP-PP1 γ 1 were co-precipitated with the myc-Nb(F-

>A) mutant (Figure 4A, lane 6). This may be due to coprecipitation of low levels of endogenous wild type neurabins in the 293FT cells because a similar amount of endogenous PP1 γ 1 was immunoprecipitated with the neurabin antibody in the absence of over-expressed neurabin (Figure 4A, compare lanes 2 and 6). Most significantly, mutating the PP1 isoform selectivity domain (VK/TW) in neurabin or spinophilin resulted in a similar reduction in the co-precipitation of endogenous PP1 γ 1 and GFP-PP1 γ 1 as the canonical PP1 binding motif mutation (Figures 4A, lane 8 and 3B, lane 6). These data suggest that the canonical motif and the PP1 γ 1 selectivity determinant are equally important for PP1 γ 1 interaction with full length spinophilin or neurabin in intact cells.

To determine how these mutations affect interactions of PP1 β with spinophilin in cells, we co-expressed wild type or mutated spinophilin with GFP-PP1 β and immunoprecipitated spinophilin from the cell extracts. Immunoblotting using GFP antibodies detected GFP-PP1 β in myc-Sp(WT) immune complexes, but the levels of GFP-PP1 β were apparently lower than those of GFP-PP1 γ 1 in parallel immunoprecipitations (Figure 4C, compare lanes 2 and 8). Moreover, although myc-neurabin(WT) and myc-spinophilin(WT) immunoprecipitates contained endogenous PP1 γ 1 in addition to GFP-PP1 γ 1 (Fig. 4A/B), we failed to detect endogenous HEK293 cell PP1 β using our PP1 β antibodies (data not shown), consistent with prior studies showing that PP1 β is not significantly associated with spinophilin or neurabin in brain (13). These data show that full-length spinophilin displays a similar preference for co-expressed GFP-PP1 and endogenous HEK293 cell PP1 isoforms as do neurabin fragments for purified brain PP1 isoforms *in vitro* (Figures 2C and 3). Mutation of the canonical PP1 binding motif (myc-Sp(F->A)) appeared to abrogate the co-precipitation of GFP-PP1 β . However, GFP-PP1 β was readily detected in myc-Sp(VK/TW) immune complexes using antibodies to GFP (Figure 4C, lanes 4 and 6). In fact, we detected a similar ratio of GFP-PP1 β to myc-spinophilin in myc immune complexes isolated from cells expressing the wild type or VK/TW mutated proteins. Taken together, these data demonstrate that in the context of full length protein in intact cells the canonical PP1-binding motifs in neurabin and spinophilin are important for binding both isoforms, whereas the selectivity determinant only affects association of PP1 γ 1.

Effect of PP1-binding site mutations on PP1 isoform targeting

In order to better understand the mechanisms underlying neurabins modulation of PP1 isoform localization, we used two different approaches to quantify GFP-PP1 isoform targeting to F-actin from fluorescent images. GFP-PP1 isoforms were co-expressed with myc-spinophilin (wild type or mutated) and rhodamine-phalloidin was used to stain F-actin. Importantly, we chose HEK293 cells for these studies because these transfections had little effect on cell size and morphology under our culture conditions (Fig. 1), thus avoiding potentially misleading effects due to morphological changes. Images of random fields from each transfection were collected using identical microscope settings in order to avoid potential operator bias in selecting individual cells. Consistent with data in Fig. 1B, immunofluorescence signals for myc-Sp(WT) strongly overlapped rhodamine-phalloidin fluorescence in the cortical region of transfected cells, confirming previous studies showing that neurabins associate with F-actin rich structures in numerous cell types. In the absence of myc-Sp(WT), GFP-PP1 γ 1 fluorescence clustered in the center of cells and clearly did not strongly overlap with F-actin cytoskeletal elements (rhodamine-phalloidin) (Fig. 5A); in fact, only \approx 15% of GFP-PP1 γ 1 positive pixels overlapped with rhodamine phalloidin-positive pixels (Figure 5B). Co-expression of myc-Sp(WT) resulted in a dramatic re-distribution of GFP-PP1 γ 1 to the cell periphery such that GFP-PP1 γ 1 colocalized with both myc-Sp(WT) and the F-actin cytoskeleton in the transfected cells: \approx 70% of GFP-PP1 γ 1 positive pixels overlapped with rhodamine phalloidin in the presence of myc-spinophilin(WT), representing an \approx 5-fold increase in PP1 γ 1 targeting to F-actin by myc-spinophilin(WT). However, these pixel overlap scores do not take into account the relative strength of GFP signals in the two subcellular compartments (phalloidin vs. non-phalloidin).

Therefore, we also quantified the ratio of GFP fluorescence intensity in F-actin-localized versus non-F-actin-localized pools, as defined by the presence or absence of rhodamine-phalloidin fluorescence. By this measure, myc-Sp(WT) enhanced the localization of GFP-PP1 γ 1 to F-actin by \approx 18-fold. In combination, these two semi-quantitative measures show for the first time that spinophilin targets PP1 γ 1 to F-actin in intact cells.

Similar studies were performed with GFP-PP1 β in order to examine the isoform selectivity of PP1 targeting by spinophilin in intact cells. In the absence of myc-spinophilin, GFP-PP1 β was relatively diffusely localized throughout the cell (Figure 5C), consistent with Fig. 1A, such that it was not distinctly excluded from the F-actin cytoskeleton. This was reflected in somewhat higher colocalization scores by both Pixel Overlap and Intensity Ratio measures than observed when GFP-PP1 γ 1 was expressed alone (\approx 35% and \approx 0.5 vs. \approx 15% and \approx 0.1 for GFP-PP1 β and GFP-PP1 γ 1, respectively). Co-expression of myc-Sp(WT) resulted in a significant, but much more subtle, enrichment of GFP-PP1 β at the F-actin cytoskeleton, compared to the dramatic redistribution of GFP-PP1 γ 1 induced by myc-Sp(WT) (compare Figure 5A/C). Although myc-spinophilin(WT)-enhanced F-actin localization of GFP-PP1 β was statistically significant by both Pixel Overlap and Intensity Ratio measures, there was only an \approx 2-fold increased enrichment of GFP-PP1 β at F-actin (Figure 5D), compared to the \approx 18-fold enrichment of GFP-PP1 γ 1, representing a 9-fold selectivity for GFP-PP1 γ 1 by this measure. Thus, the combined data show that spinophilin selectively targets PP1 γ 1 to the F-actin cytoskeleton in intact cells.

The importance of different domains in spinophilin for PP1 targeting was then determined by co-expressing GFP-tagged PP1 isoforms with spinophilins containing mutations in the canonical PP1-binding motif (myc-Sp(F->A)) or in the PP1 γ 1 selectivity determinant (myc-Sp(VK/TW)). Neither mutation had a noticeable effect on F-actin-targeting of spinophilin itself (blue channels in Figures 5A), but both disrupted the localization of GFP-PP1 γ 1 to the F-actin cytoskeleton in a similar manner. In both cases, a fraction of GFP-PP1 γ 1 co-localized with the mutated proteins and rhodamine-phalloidin at the cell periphery, but GFP-PP1 γ 1 fluorescence was prominent in central intracellular clusters (Figure 5A), similar to those observed in the absence of myc-Sp (c.f., Figure 1). Quantitative measures of the pixel overlap and fluorescence intensity ratios revealed that mutation of the canonical motif or the PP1 γ 1 selectivity determinant partially disrupted F-actin targeting of GFP-PP1 γ 1 to a similar extent (Figure 5B). In contrast, the modest enhancement of F-actin targeting of GFP-PP1 β by myc-Sp(WT) was sensitive to mutation of the canonical motif, but not to mutation in the C-terminal selectivity determinant (Figure 5C/D). In combination, these data show that the canonical PP1-binding motif in spinophilin is critical for interactions with both PP1 isoforms in intact cells. However, a domain C-terminal to this motif (residues 473–479) is also critical for the selective and strong targeting of GFP-PP1 γ 1 to F-actin.

Discussion

Dendritic spines are highly enriched with F-actin and F-actin regulatory proteins such as neurabin, spinophilin, and PP1 γ 1 (4–6,11,12,14,15). N-terminal F-actin-binding domains target spinophilin and neurabin to dendritic spines (11,12,32,33). Previous studies have suggested that interactions of several other proteins with neurabins modulate F-actin dynamics and cell morphology (e.g., (21,34)). In addition, cell morphology and dendritic spine dynamics are affected by interactions of undefined PP1 isoforms with over-expressed truncated neurabin fragments (32,35), although the physiological relevance of these observations is unclear. PP1 targeting by neurabins also is important for normal regulation of synaptic and extrasynaptic AMPA and NMDA-type glutamate receptors (7,9,36). While these studies infer an important role for PP1 binding to neurabins *in situ*, subcellular targeting of PP1 by the neurabins has not been directly demonstrated, and the isoform selectivity of targeting is not clearly defined. Here

we examine the targeting of PP1 isoforms to F-actin in HEK293 cells, which are relatively resistant to morphological changes induced by our experimental manipulations, thus avoiding potential complications in experimental interpretation. Our data show that spinophilin selectively targets PP1 γ 1 over PP1 β to F-actin in intact cells and identify specific amino acids in an auxiliary interaction domain that are required for selective targeting.

The neurabins contain a canonical R/K-V/I-X-F/W PP1-binding motif and structures of PP1 catalytic subunits bound to proteins/peptides containing this motif have been elucidated (37–39). Variants of the canonical motif exhibit different affinities for PP1. Mutagenesis studies with mGluR7b and inhibitor-1 suggest that Ile may confer a lower affinity interaction than Val at the V/I position (38,40). In contrast, exchanging neurabin's motif (KIKF) for that of G_M (RVSF) attenuated PP1 binding (26). This discrepancy may reflect different sequence contexts of the canonical motifs and/or the presence of different auxiliary interactions (see below). Alternatively, it may reflect the use of different sources of PP1 isoforms. We studied interactions with native PP1 isoforms because recombinant proteins expressed in bacteria typically do not exhibit the full repertoire of native enzymatic functions (31). Most significantly in this context, native brain PP1 γ 1 is inhibited by GST-Nb(146–493) \approx 100-fold more potently than is recombinant PP1 γ 1 from bacteria (29). One interesting aspect of the present studies is that the magnitude of the effect of the F->A mutation in the canonical PP1-binding motif depends on the assay used to monitor the interactions. The F->A mutation appears to almost completely block the interaction in pull-down and co-immunoprecipitation assays that require extensive washing to remove excess unbound PP1 from the complexes (Figs. 2, 4). In contrast, it is clear from activity and colocalization assays that monitor steady state interaction that the F->A mutant neurabins retain significant interactions with PP1 (Figs. 3, 5). It is likely that higher protein concentrations, combined with the lack of washing to remove unbound PP1, allows for detection of the residual weak interactions in enzyme activity assays and in intact cells. These data suggest caution in interpreting data obtained by comparing effects of wild-type PP1-binding proteins with F->A mutated proteins as revealing a functional role (or lack thereof) for the PP1 interaction. More extensive mutations of the canonical motif might be required to completely block PP1 binding in intact cells. Despite these differences, our data are consistent with the consensus view that the Phe residue within the canonical motif is critical for high affinity PP1 binding and that the canonical motif does not influence PP1 isoform selectivity.

Canonical PP1-binding motifs may provide an anchor to facilitate auxiliary secondary interactions between PP1 and its targeting/regulatory subunits (2). For example, the auxiliary domains in DARPP-32 and inhibitor-1 contain PKA phosphorylation sites, allowing the phosphorylated proteins to potently inhibit PP1 (41–43). Similarly, the myosin targeting subunit (MYPT) contains a structural domain that has extensive secondary interactions with the C-terminal domain of PP1 β (39). Previous studies showed that residues N-terminal to the canonical motif stabilize weak interactions of neurabin with PP1 β (25). In contrast, analysis of chimeric proteins containing domains from neurabin and G_M, the PP1 β -selective glycogen targeting subunit, showed that residues C-terminal to the canonical motif are critical for overall PP1 γ 1 selectivity *in vitro*, and this idea was supported by truncation mutagenesis studies that specifically implicated residues 473–479 as a PP1 γ 1 selectivity determinant (26). Here, we identified specific amino acids in neurabin and spinophilin that are important for high affinity, selective interactions with PP1 γ 1 *in vitro* and show that these same residues are important in the selective targeting of PP1 γ 1 in cells. Comparison of amino acid sequences surrounding the canonical PP1-binding motifs in neurabins and G_M revealed weak overall similarity, with the exception of a cluster of residues overlapping the putative PP1 γ 1 selectivity determinant that are 70% identical. Notably, four amino acids in neurabin within the putative PP1 γ 1 selectivity determinant (Asn⁴⁷³, Glu⁴⁷⁴, Arg⁴⁷⁸, Arg⁴⁷⁹) are identical in spinophilin but are not conserved in G_M (Figure 2A). Mutating neurabin residues 473, 474, 478 and 479 to the corresponding

residues from G_M (VK/TW mutant), disrupted PP1 γ 1 binding to fragments of neurabin *in vitro*, but had little to no effect on PP1 β binding (Figs. 2 and 3). In the context of both full length neurabin and full length spinophilin the corresponding VK/TW mutation strongly affected association of PP1 γ 1 in co-immunoprecipitation assays, but had little to no effect on the much weaker association of GFP-PP1 β . Moreover, the VK/TW mutation substantially reduced the selective targeting of PP1 γ 1 to F-actin with no detectable effect on the much weaker targeting of GFP-PP1 β . Thus, residues 473–479 of neurabin and residues 464–470 of spinophilin are critical for PP1 γ 1 selective binding to neurabins *in vitro* and in intact cells.

In combination, our results suggest a model in which at least two domains in the neurabins are needed for selective targeting of PP1 γ 1 to F-actin in intact cells. The canonical PP1-binding motif can interact with both PP1 isoforms, but an auxiliary selectivity determinant strongly stabilizes binding of PP1 γ 1, but not PP1 β , accounting for selective targeting (Figure 6, top row). Mutation of the canonical motif weakens interactions with both isoforms such that the selectivity ratio is unchanged, presumably because the PP1 γ 1 selectivity determinant is intact (Figure 6, middle row). Lastly, mutation of the selectivity determinant in either neurabin or spinophilin disrupts binding of PP1 γ 1, but does not affect binding of PP1 β , thereby abrogating selectivity (Figure 6, bottom row).

Although the NE/RR motif is completely conserved in all mammalian neurabins, it is unclear whether other PP1-binding proteins employ a similar mechanism to selectively interact with PP1 γ 1 over other PP1 isoforms. In an effort to determine whether the NE/RR motif is sufficient to enhance binding of PP1 γ 1 in another context, the VK/TW residues C-terminal to the canonical PP1-binding motif in G_M were mutated to NE/RR in GST- $G_M(1-240)$. However, this mutation failed to enhance binding or inhibitory potency toward PP1 γ 1 (data not shown). Thus, the NE/RR motif may require the specific context of the neurabins in order to confer PP1 γ 1 binding selectivity. Notably, the NE/RR motif in GST- $G_M(1-240)$: NE/RR) is two amino acids closer to the canonical PP1-binding motif than the natural NE/RR motif in neurabins, and our previous studies have suggested that precise spacing between these motifs is critical for binding of PP1 γ 1 because deletion of two amino acids between the canonical PP1-binding and NE/RR selectivity motif in neurabin severely compromised PP1 γ 1 binding (26). Interestingly, inhibitor 3 displays some selectivity for PP1 γ 1 in cells (44) and also contains an **NEHMGRR** motif C-terminal to the canonical PP1-binding motif, but the spacing of the two domains is 6 residues closer than in neurabin. Thus, the functional role of this motif in the context of inhibitor 3 is unclear. No other known PP1 binding proteins appear to contain similarly located NE/RR-like motifs. These considerations lead us to suggest that employment of an NE/RR motif to confer PP1 γ 1 isoform selectivity may be contextual and relatively unique to the neurabins.

PP1 catalytic subunit isoforms exhibit similar activities *in vitro* (31), but are differentially localized in neurons and other cells (4–6,28,45,46), suggesting that they play distinct biological roles. Although interactions of PP1 α with neurabins were not investigated here due to technical limitations, previous coimmunoprecipitation data indicated that neurabins bind PP1 γ 1 > PP1 α >> PP1 β (25). Thus, it appears that spinophilin binds mostly to PP1 γ 1 in the brain, perhaps in part because PP1 γ 1 is expressed at somewhat higher levels than PP1 α (47). Interestingly, the amount of PP1 α associated with neurabins increased in PP1 γ 1 knockout mice (25). Thus, even though PP1 α and PP1 γ 1 appear to be differentially localized within spines (6), our data cannot exclude the possibility that neurabins can target both isoforms (4,6). In contrast, PP1 β is enriched in the soma and dendritic shafts where it appears to associate with microtubules (5,6).

Multiple lines of evidence suggest that neurabins mediate PP1-dependent effects on the morphology of some cells, including actin stress fiber formation, filopodia, and the development of neuronal dendrites and dendritic spines (11,32,33,35,36). The present data

suggest that PP1 γ 1 (or perhaps PP1 α), but not PP1 β , regulates signaling pathways responsible for these morphological effects by regulating protein phosphorylation/dephosphorylation in neurabin complexes. Phosphorylation of neurabins modulates binding to both PP1 and F-actin (35,48–50). Thus neurabin and additional neurabin binding partners may be dephosphorylated by bound PP1 γ 1. For example, PP1 inactivates Tiam1 (51,52), a rac-specific guanine nucleotide exchange factor that interacts with spinophilin and regulates dendritic spine development (20,53). Interestingly, Tiam1 facilitates the activation of p70 S6 kinase, another spinophilin/neurabin-associated protein that competes with PP1 for binding to neurabin (20, 35). However, despite the overall similarity between neurabin and spinophilin, recent analyses using knockout mice showed that spinophilin is critical for long-term depression, whereas neurabin is critical for long-term potentiation presumably because synaptic targeting of PP1 isoforms is critical for regulation of multiple glutamate receptors (36,54). Thus, differential targeting of PP1 isoforms by spinophilin and neurabin likely mediates distinct biological responses.

In summary, our data show that neurabins strongly target PP1 γ 1 to the F-actin cytoskeleton in intact cells, but have little effect on the localization of PP1 β . While canonical PP1 binding motifs in spinophilin and neurabin affect binding of all isoforms, a domain C-terminal to the canonical domain is essential for selective interactions with PP1 γ 1 in vitro and for selective targeting in intact cells. Thus, coordinated interactions of PP1 γ 1 with two domains in the neurabins are essential for specific targeting of PP1 γ 1 to F-actin, and presumably to dendritic spines in neurons, to facilitate dynamic modulation of the F-actin cytoskeleton, dendritic spine morphology and synaptic plasticity.

Acknowledgments

These studies were supported by NIH-PO1-NS44282. AJB was supported by the Neurogenomics Training Program (T32-MH65215). Fluorescence microscopy data were collected using the VUMC Cell Imaging Shared Resource (supported by NIH grants CA68485, DK20593, DK58404, HD15052, DK59637 and EY08126) with excellent advice from Drs. Sam Wells and Dawn Kilkenny-Rochelleau concerning quantification of images using Metamorph software. We appreciate the advice and assistance of Katherine Betke in some of the cell imaging studies. In addition, we would like to thank Dr. Brian Wadzinski, Nicole Garbarini, and Nellie Byun for their critical comments on drafts of this manuscript, as well as Dr. Ashley Brady and members of the Colbran Lab for fruitful discussions.

References

1. Ceulemans H, Bollen M. Functional diversity of protein phosphatase-1, a cellular economizer and reset button. *Physiol Rev* 2004;84:1–39. [PubMed: 14715909]
2. Bollen M. Combinatorial control of protein phosphatase-1. *Trends Biochem Sci* 2001;26:426–431. [PubMed: 11440854]
3. Cohen PT. Protein phosphatase 1--targeted in many directions. *J Cell Sci* 2002;115:241–256. [PubMed: 11839776]
4. Ouimet CC, da Cruz e Silva EF, Greengard P. The alpha and gamma 1 isoforms of protein phosphatase 1 are highly and specifically concentrated in dendritic spines. *Proc Natl Acad Sci USA* 1995;92:3396–3400. [PubMed: 7724573]
5. Strack S, Kini S, Ebner FF, Wadzinski BE, Colbran RJ. Differential cellular and subcellular localization of protein phosphatase 1 isoforms in brain. *J Comp Neurol* 1999;413:373–384. [PubMed: 10502246]
6. Bordelon JR, Smith Y, Nairn AC, Colbran RJ, Greengard P, Muly EC. Differential localization of protein phosphatase-1alpha, beta and gamma1 isoforms in primate prefrontal cortex. *Cereb Cortex* 2005;15:1928–1937. [PubMed: 15758197]
7. Yan Z, Hsieh-Wilson L, Feng J, Tomizawa K, Allen PB, Fienberg AA, Nairn AC, Greengard P. Protein phosphatase 1 modulation of neostriatal AMPA channels: regulation by DARPP-32 and spinophilin. *Nat Neurosci* 1999;2:13–17. [PubMed: 10195174]
8. Morishita W, Connor JH, Xia H, Quinlan EM, Shenolikar S, Malenka RC. Regulation of synaptic strength by protein phosphatase 1. *Neuron* 2001;32:1133–1148. [PubMed: 11754843]

9. Hu XD, Huang Q, Roadcap DW, Shenolikar SS, Xia H. Actin-associated neurabin-protein phosphatase-1 complex regulates hippocampal plasticity. *J Neurochem* 2006;98:1841–1851. [PubMed: 16899074]
10. Allen PB, Ouimet CC, Greengard P. Spinophilin, a novel protein phosphatase 1 binding protein localized to dendritic spines. *Proc Natl Acad Sci USA* 1997;94:9956–9961. [PubMed: 9275233]
11. Nakanishi H, Obaishi H, Satoh A, Wada M, Mandai K, Satoh K, Nishioka H, Matsuura Y, Mizoguchi A, Takai Y. Neurabin: a novel neural tissue-specific actin filament-binding protein involved in neurite formation. *J Cell Biol* 1997;139:951–961. [PubMed: 9362513]
12. Satoh A, Nakanishi H, Obaishi H, Wada M, Takahashi K, Satoh K, Hirao K, Nishioka H, Hata Y, Mizoguchi A, Takai Y. Neurabin-II/spinophilin. An actin filament-binding protein with one pdz domain localized at cadherin-based cell-cell adhesion sites. *J Biol Chem* 1998;273:3470–3475. [PubMed: 9452470]
13. MacMillan LB, Bass MA, Cheng N, Howard EF, Tamura M, Strack S, Wadzinski BE, Colbran RJ. Brain actin-associated protein phosphatase 1 holoenzymes containing spinophilin, neurabin, and selected catalytic subunit isoforms. *J Biol Chem* 1999;274:35845–35854. [PubMed: 10585469]
14. Muly EC, Allen P, Mazloom M, Aranbayeva Z, Greenfield AT, Greengard P. Subcellular distribution of neurabin immunolabeling in primate prefrontal cortex: comparison with spinophilin. *Cereb Cortex* 2004;14:1398–1407. [PubMed: 15217898]
15. Muly EC, Smith Y, Allen P, Greengard P. Subcellular distribution of spinophilin immunolabeling in primate prefrontal cortex: localization to and within dendritic spines. *J Comp Neurol* 2004;469:185–197. [PubMed: 14694533]
16. Ouimet CC, Katona I, Allen P, Freund TF, Greengard P. Cellular and subcellular distribution of spinophilin, a PP1 regulatory protein that bundles F-actin in dendritic spines. *J Comp Neurol* 2004;479:374–388. [PubMed: 15514983]
17. Burnett PE, Blackshaw S, Lai MM, Qureshi IA, Burnett AF, Sabatini DM, Snyder SH. Neurabin is a synaptic protein linking p70 S6 kinase and the neuronal cytoskeleton. *Proc Natl Acad Sci USA* 1998;95:8351–8356. [PubMed: 9653190]
18. Smith FD, Oxford GS, Milgram SL. Association of the D2 dopamine receptor third cytoplasmic loop with spinophilin, a protein phosphatase-1-interacting protein. *J Biol Chem* 1999;274:19894–19900. [PubMed: 10391935]
19. Richman JG, Brady AE, Wang Q, Hensel JL, Colbran RJ, Limbird LE. Agonist-regulated Interaction between alpha2-adrenergic receptors and spinophilin. *J Biol Chem* 2001;276:15003–15008. [PubMed: 11154706]
20. Buchsbaum RJ, Connolly BA, Feig LA. Regulation of p70 S6 kinase by complex formation between the Rac guanine nucleotide exchange factor (Rac-GEF) Tiam1 and the scaffold spinophilin. *J Biol Chem* 2003;278:18833–18841. [PubMed: 12531897]
21. Ryan XP, Alldritt J, Svenningsson P, Allen PB, Wu GY, Nairn AC, Greengard P. The Rho-specific GEF Lfc interacts with neurabin and spinophilin to regulate dendritic spine morphology. *Neuron* 2005;47:85–100. [PubMed: 15996550]
22. Wang X, Zeng W, Soyombo AA, Tang W, Ross EM, Barnes AP, Milgram SL, Penninger JM, Allen PB, Greengard P, Muallem S. Spinophilin regulates Ca²⁺ signalling by binding the N-terminal domain of RGS2 and the third intracellular loop of G-protein-coupled receptors. *Nat Cell Biol* 2005;7:405–411. [PubMed: 15793568]
23. Sarrouilhe D, di Tommaso A, Metaye T, Ladeveze V. Spinophilin: from partners to functions. *Biochimie* 2006;88:1099–1113. [PubMed: 16737766]
24. Hsieh-Wilson LC, Allen PB, Watanabe T, Nairn AC, Greengard P. Characterization of the neuronal targeting protein spinophilin and its interactions with protein phosphatase-1. *Biochemistry* 1999;38:4365–4373. [PubMed: 10194355]
25. Terry-Lorenzo RT, Carmody LC, Voltz JW, Connor JH, Li S, Smith FD, Milgram SL, Colbran RJ, Shenolikar S. The neuronal actin-binding proteins, neurabin I and neurabin II, recruit specific isoforms of protein phosphatase-1 catalytic subunits. *J Biol Chem* 2002;277:27716–27724. [PubMed: 12016225]

26. Carmody LC, Bauman PA, Bass MA, Mavila N, DePaoli-Roach AA, Colbran RJ. A protein phosphatase-1gamma1 isoform selectivity determinant in dendritic spine-associated neurabin. *J Biol Chem* 2004;279:21714–21723. [PubMed: 15016827]
27. Zheng L, Baumann U, Reymond JL. An efficient one-step site-directed and site-saturation mutagenesis protocol. *Nucleic Acids Res* 2004;32:e115. [PubMed: 15304544]
28. Lesage B, Beullens M, Nuytten M, Van Eynde A, Keppens S, Himpens B, Bollen M. Interactor-mediated nuclear translocation and retention of protein phosphatase-1. *J Biol Chem* 2004;279:55978–55984. [PubMed: 15501817]
29. Colbran RJ, Carmody LC, Bauman PA, Wadzinski BE, Bass MA. Analysis of specific interactions of native protein phosphatase 1 isoforms with targeting subunits. *Methods Enzymol* 2003;366:156–175. [PubMed: 14674248]
30. Lanner C, Suzuki Y, Bi C, Zhang H, Cooper LD, Bowker-Kinley MM, DePaoli-Roach AA. Gene structure and expression of the targeting subunit, RGL, of the muscle-specific glycogen-associated type 1 protein phosphatase, PP1G. *Archives of biochemistry and biophysics* 2001;388:135–145. [PubMed: 11361130]
31. Alessi DR, Street AJ, Cohen P, Cohen PT. Inhibitor-2 functions like a chaperone to fold three expressed isoforms of mammalian protein phosphatase-1 into a conformation with the specificity and regulatory properties of the native enzyme. *Eur J Biochem* 1993;213:1055–1066. [PubMed: 8389292]
32. Terry-Lorenzo RT, Roadcap DW, Otsuka T, Blanpied TA, Zamorano PL, Garner CC, Shenolikar S, Ehlers MD. Neurabin/protein phosphatase-1 complex regulates dendritic spine morphogenesis and maturation. *Mol Biol Cell* 2005;16:2349–2362. [PubMed: 15743906]
33. Zito K, Knott G, Shepherd GM, Shenolikar S, Svoboda K. Induction of spine growth and synapse formation by regulation of the spine actin cytoskeleton. *Neuron* 2004;44:321–334. [PubMed: 15473970]
34. Tsukada M, Prokscha A, Ungewickell E, Eichele G. Doublecortin association with actin filaments is regulated by neurabin II. *J Biol Chem* 2005;280:11361–11368. [PubMed: 15632197]
35. Oliver CJ, Terry-Lorenzo RT, Elliott E, Bloomer WA, Li S, Brautigam DL, Colbran RJ, Shenolikar S. Targeting protein phosphatase 1 (PP1) to the actin cytoskeleton: the neurabin I/PP1 complex regulates cell morphology. *Mol Cell Biol* 2002;22:4690–4701. [PubMed: 12052877]
36. Feng J, Yan Z, Ferreira A, Tomizawa K, Liauw JA, Zhuo M, Allen PB, Ouimet CC, Greengard P. Spinophilin regulates the formation and function of dendritic spines. *Proc Natl Acad Sci USA* 2000;97:9287–9292. [PubMed: 10922077]
37. Egloff MP, Johnson DF, Moorhead G, Cohen PT, Cohen P, Barford D. Structural basis for the recognition of regulatory subunits by the catalytic subunit of protein phosphatase 1. *EMBO J* 1997;16:1876–1887. [PubMed: 9155014]
38. Meiselbach H, Sticht H, Enz R. Structural analysis of the protein phosphatase 1 docking motif: molecular description of binding specificities identifies interacting proteins. *Chem Biol* 2006;13:49–59. [PubMed: 16426971]
39. Terrak M, Kerff F, Langsetmo K, Tao T, Dominguez R. Structural basis of protein phosphatase 1 regulation. *Nature* 2004;429:780–784. [PubMed: 15164081]
40. Wakula P, Beullens M, Ceulemans H, Stalmans W, Bollen M. Degeneracy and function of the ubiquitous RVXF motif that mediates binding to protein phosphatase-1. *J Biol Chem* 2003;278:18817–18823. [PubMed: 12657641]
41. Endo S, Zhou X, Connor J, Wang B, Shenolikar S. Multiple structural elements define the specificity of recombinant human inhibitor-1 as a protein phosphatase-1 inhibitor. *Biochemistry* 1996;35:5220–5228. [PubMed: 8611507]
42. Hemmings HC Jr, Nairn AC, Elliott JI, Greengard P. Synthetic peptide analogs of DARPP-32 (Mr 32,000 dopamine- and cAMP-regulated phosphoprotein), an inhibitor of protein phosphatase-1. Phosphorylation, dephosphorylation, and inhibitory activity. *J Biol Chem* 1990;265:20369–20376. [PubMed: 2173704]
43. Yang J, Hurley TD, DePaoli-Roach AA. Interaction of inhibitor-2 with the catalytic subunit of type 1 protein phosphatase. Identification of a sequence analogous to the consensus type 1 protein phosphatase-binding motif. *J Biol Chem* 2000;275:22635–22644. [PubMed: 10807923]

44. Huang HS, Pozarowski P, Gao Y, Darzynkiewicz Z, Lee EY. Protein phosphatase-1 inhibitor-3 is co-localized to the nucleoli and centrosomes with PP1 gamma1 and PP1 alpha, respectively. *Archives of biochemistry and biophysics* 2005;443:33–44. [PubMed: 16256067]
45. Trinkle-Mulcahy L, Sleeman JE, Lamond AI. Dynamic targeting of protein phosphatase 1 within the nuclei of living mammalian cells. *J Cell Sci* 2001;114:4219–4228. [PubMed: 11739654]
46. Haneji T, Morimoto H, Morimoto Y, Shirakawa S, Kobayashi S, Kaneda C, Shima H, Nagao M. Subcellular localization of protein phosphatase type 1 isotypes in mouse osteoblastic cells. *Biochem Biophys Res Commun* 1998;248:39–43. [PubMed: 9675082]
47. Shima H, Hatano Y, Chun YS, Sugimura T, Zhang Z, Lee EY, Nagao M. Identification of PP1 catalytic subunit isotypes PP1 gamma 1, PP1 delta and PP1 alpha in various rat tissues. *Biochem Biophys Res Commun* 1993;192:1289–1296. [PubMed: 7685164]
48. McAvoy T, Allen PB, Obaishi H, Nakanishi H, Takai Y, Greengard P, Nairn AC, Hemmings HC Jr. Regulation of neurabin I interaction with protein phosphatase 1 by phosphorylation. *Biochemistry* 1999;38:12943–12949. [PubMed: 10504266]
49. Hsieh-Wilson LC, Benfenati F, Snyder GL, Allen PB, Nairn AC, Greengard P. Phosphorylation of spinophilin modulates its interaction with actin filaments. *J Biol Chem* 2003;278:1186–1194. [PubMed: 12417592]
50. Grossman SD, Futter M, Snyder GL, Allen PB, Nairn AC, Greengard P, Hsieh-Wilson LC. Spinophilin is phosphorylated by Ca²⁺/calmodulin-dependent protein kinase II resulting in regulation of its binding to F-actin. *J Neurochem* 2004;90:317–324. [PubMed: 15228588]
51. Buchanan FG, Elliot CM, Gibbs M, Exton JH. Translocation of the Rac1 guanine nucleotide exchange factor Tiam1 induced by platelet-derived growth factor and lysophosphatidic acid. *J Biol Chem* 2000;275:9742–9748. [PubMed: 10734127]
52. Fleming IN, Elliott CM, Buchanan FG, Downes CP, Exton JH. Ca²⁺/calmodulin-dependent protein kinase II regulates Tiam1 by reversible protein phosphorylation. *J Biol Chem* 1999;274:12753–12758. [PubMed: 10212259]
53. Toliaas KF, Bikoff JB, Burette A, Paradis S, Harrar D, Tavazoie S, Weinberg RJ, Greenberg ME. The Rac1-GEF Tiam1 couples the NMDA receptor to the activity-dependent development of dendritic arbors and spines. *Neuron* 2005;45:525–538. [PubMed: 15721239]
54. Allen PB, Zachariou V, Svenningsson P, Lepore AC, Centonze D, Costa C, Rossi S, Bender G, Chen G, Feng J, Snyder GL, Bernardi G, Nestler EJ, Yan Z, Calabresi P, Greengard P. Distinct roles for spinophilin and neurabin in dopamine-mediated plasticity. *Neuroscience* 2006;140:897–911. [PubMed: 16600521]

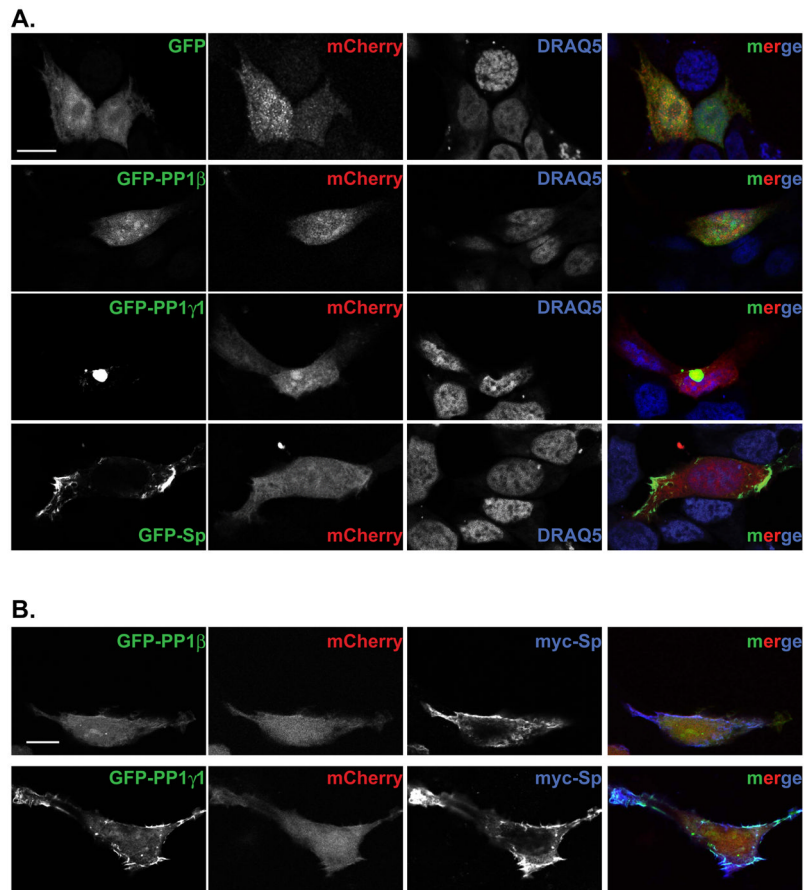


Figure 1. Preferential targeting of GFP-PP1 γ 1 by spinophilin in intact cells. **A.** HEK293 cells were transfected to co-express mCherry with eGFP or the indicated eGFP fusion proteins. Cells were fixed and counter stained with DRAQ5, a nuclear stain. Confocal microscope images of the intrinsic fluorescence of GFP, mCherry and DRAQ5 are shown on a grayscale, with the last column representing an overlay of all three channels in the green, red and blue channels, respectively. **B.** HEK293 cells were transfected to express myc-spinophilin and mCherry with either GFP-PP1 β or GFP-PP1 γ 1. Fixed cells were processed to detect myc immunofluorescence (blue) and intrinsic GFP (green) or mCherry (red) fluorescence by confocal microscopy as in panel A. Scale bars in top left images of panels A and B applies to all images in that panel.

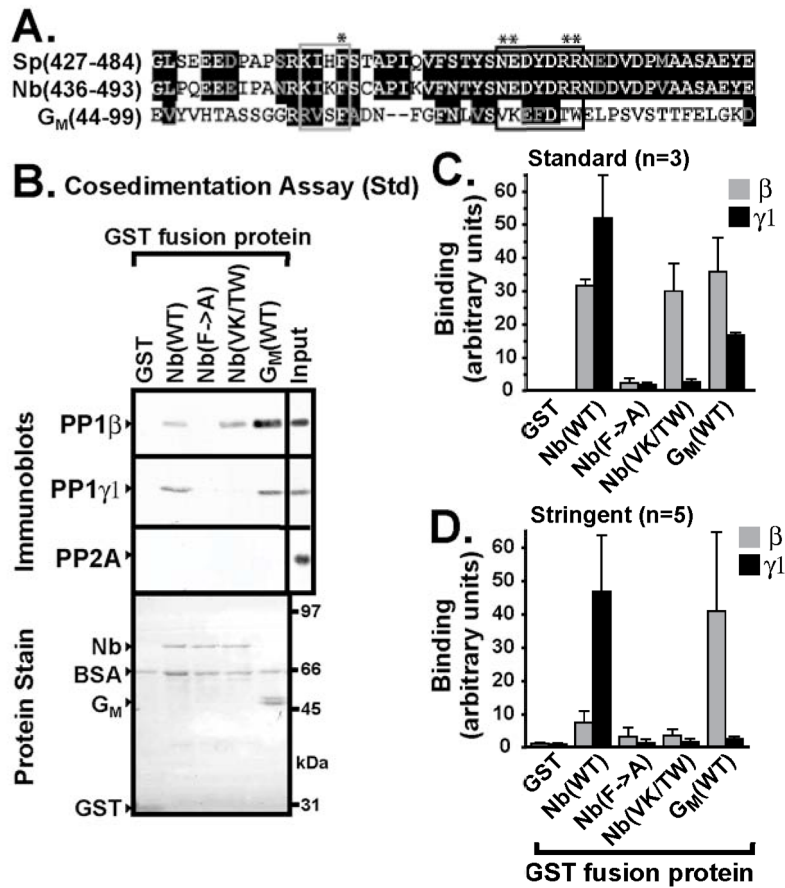


Figure 2. Effects of mutagenesis on PP1 binding to neurabin fragments. **A.** Alignment of sequences surrounding the canonical PP1-binding motif (R/K-V/I-X-F/W, grey box) in neurabin/spinophilin and G_M. Identical and conserved amino acids are indicated in black boxes (white and gray letters, respectively). The black rectangle outlines a cluster of residues C-terminal to the canonical motif that overlap a domain previously shown to be essential for PP1γ1-selective interactions by truncation mutagenesis (26). Residues marked with asterisks were targeted by site directed mutagenesis in the present studies (see text). **(B–D)** The indicated GST fusion proteins (8 μg) were incubated with a crude protein phosphatase catalytic subunit mixture (15 μg of total protein) under “standard” conditions (**B** and **C**, 1 ml) or “stringent” conditions (**D**, 14 ml) (see Methods). The resulting complexes were collected using glutathione agarose and immunoblotted for PP1β, PP1γ1, and PP2A. A sample of the protein phosphatase catalytic subunit mixture was analyzed in parallel (Input). Prior to immunoblotting, nitrocellulose membranes were stained with Ponceau to reveal the amounts of GST fusion protein in each lane (Protein stain): the arrowhead labeled “BSA” marks bovine serum albumin carried over from the incubation buffer. **(B)** Representative raw data obtained under “standard” conditions. **(C)** Quantification of three separate experiments performed under “standard” conditions. **(D)** Quantification of five separate experiments performed under “Stringent” conditions. Bars represent the mean ± SEM.

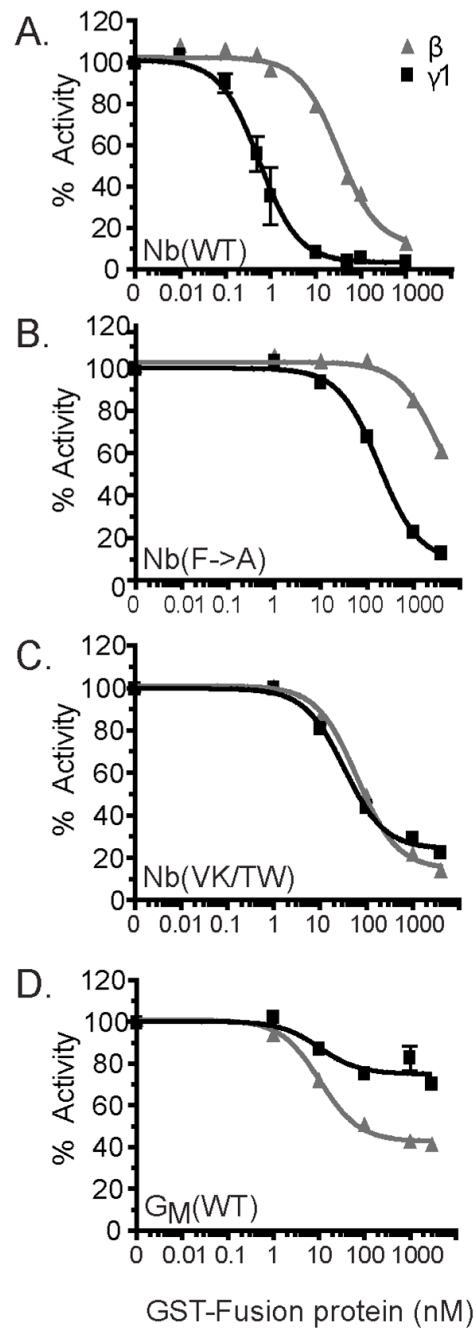


Figure 3.

Effects of mutagenesis on inhibition of native PP1 isoforms by neurabin fragments. Activities of native PP1 β (gray lines/triangles) and PP1 γ 1 (black lines/squares) were assayed in the presence of the various concentrations of the indicated GST fusion proteins. Each data point represents mean \pm SEM of 2–5 observations. GST alone (3 μ M) had no significant effect on PP1 β or PP1 γ 1 (data not shown).

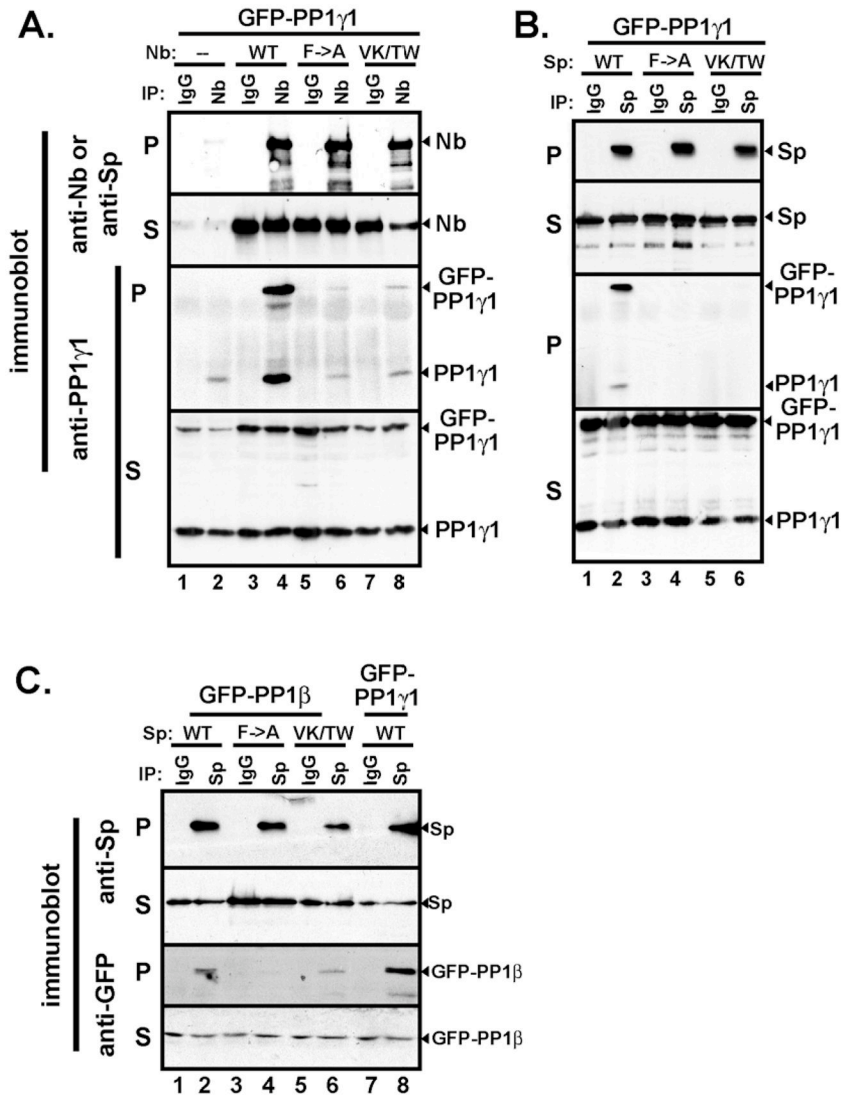


Figure 4. Effects of mutagenesis on PP1-binding to full-length neurabin and spinophilin in intact cells. Soluble extracts of 293FT cells expressing GFP-PP1 γ 1, GFP-PP1 β , and/or myc-tagged, full-length neurabins (wild type or containing the indicated mutations) were immunoprecipitated (IP) using rabbit antibodies to neurabin (Nb) or spinophilin (Sp), or using equivalent amounts of control rabbit IgG (IgG). Immune complexes (P) and supernatants (S) were immunoblotted with mouse antibodies to neurabin, spinophilin or GFP or sheep antibodies to PP1 γ 1 (PP1 γ 1 blots in panels A and B show an approximate molecular weight range from 31 kDa at the bottom to 66kDa at the top). **(A)** Cells expressing GFP-PP1 γ 1 with or without wild-type or mutated neurabin. **(B)** Cells expressing GFP-PP1 γ 1 with wild-type or mutated spinophilin. **(C)** Cells expressing GFP-PP1 β or GFP-PP1 γ 1 with wild-type or mutated spinophilin.

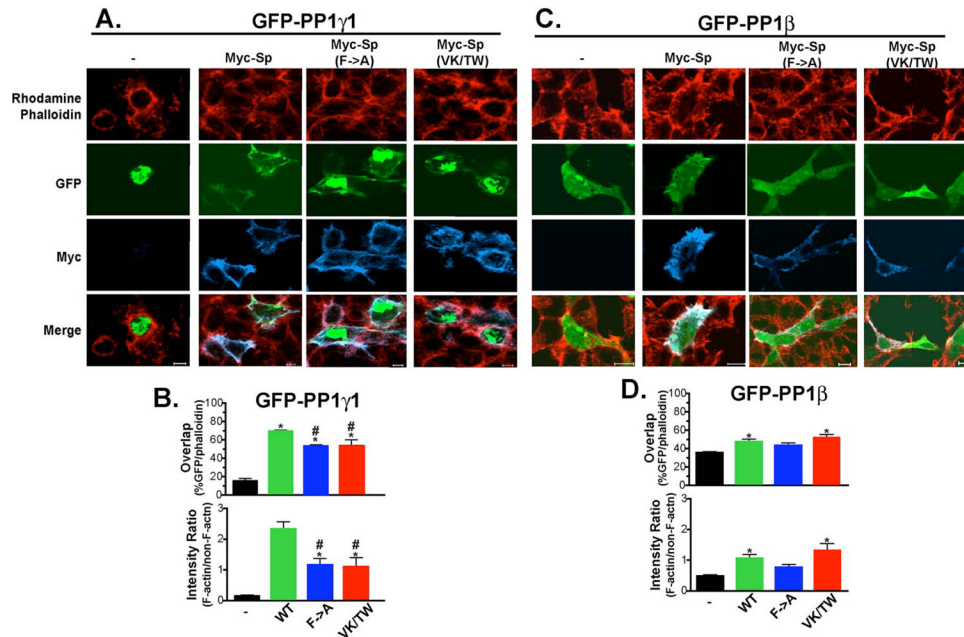


Figure 5. The canonical PP1-binding motif and the selectivity determinant are required for selective targeting of GFP-PP1 γ to F-actin. **(A)** Coexpression of GFP-PP1 γ 1 and wild type or mutated spinophilin in 293FT cells. Cells expressing GFP-PP1 γ 1 without or with the indicated myc-spinophilin were fixed and stained with rhodamine-phalloidin (red). Antibodies to the myc epitope were used to detect spinophilin (blue) and GFP was detected by autofluorescence (green). White scale bars in merged images indicate 10 μ m. **(B)** Quantification of colocalization of GFP-PP1 γ 1 with F-actin. *Top panel:* Percentage colocalization scores are the fraction of GFP containing pixels that overlap with rhodamine-phalloidin pixels, providing a colocalization measurement that is independent of relative signal intensity. *Bottom panel:* The intensity ratio is the ratio of GFP fluorescence intensity in pixels that overlap with rhodamine to GFP fluorescence intensity in pixels that do not overlap with rhodamine. **(C)** Coexpression of GFP-PP1 β and wild type spinophilin in 293FT cells. Cells expressing GFP-PP1 β without or with wild type myc-spinophilin were fixed, stained and imaged as for panel A. **(D)** Quantification of colocalization of GFP-PP1 β with F-actin. See panel B for details. Data are plotted as mean \pm SEM and were analyzed by one-way ANOVA using Bonferroni post-hoc tests. Asterisks (*) indicate conditions significantly different from the GFP-PP1 isoform alone ($p < 0.05$) and number signs (#) indicate conditions significantly different from cotransfection of GFP-PP1 γ 1 and spinophilin(WT) ($p < 0.05$).

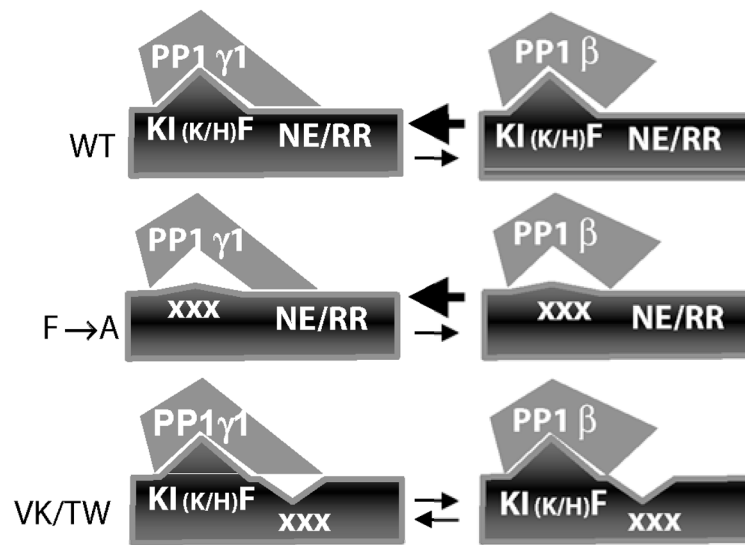


Figure 6. Working model of PP1 interactions with neurabin/spinophilin. Neurabin/spinophilin associates with PP1 γ 1 via a canonical binding motif (KI(K/H)F) and a PP1 γ 1-selectivity determinant (NE/RR). “XXX” indicates mutations of each motif. The weight of the arrows in each row indicates the relative binding of PP1 γ 1 and PP1 β to each form of spinophilin. See text for details.